



# Free-Form Motion Control: A Synthetic Video Generation Dataset with Controllable Camera and Object Motions

Xincheng Shuai<sup>1</sup> Henghui Ding<sup>1</sup> Zhenyuan Qin<sup>1</sup> Hao Luo<sup>2</sup> Xingjun Ma<sup>1</sup> Dacheng Tao<sup>3</sup>  
<sup>1</sup>Fudan University <sup>2</sup>DAMO Academy, Alibaba Group <sup>3</sup>Nanyang Technological University  
<https://henghuiding.github.io/SynFMC>

arXiv:2501.01425v2 [cs.CV] 3 Jan 2025

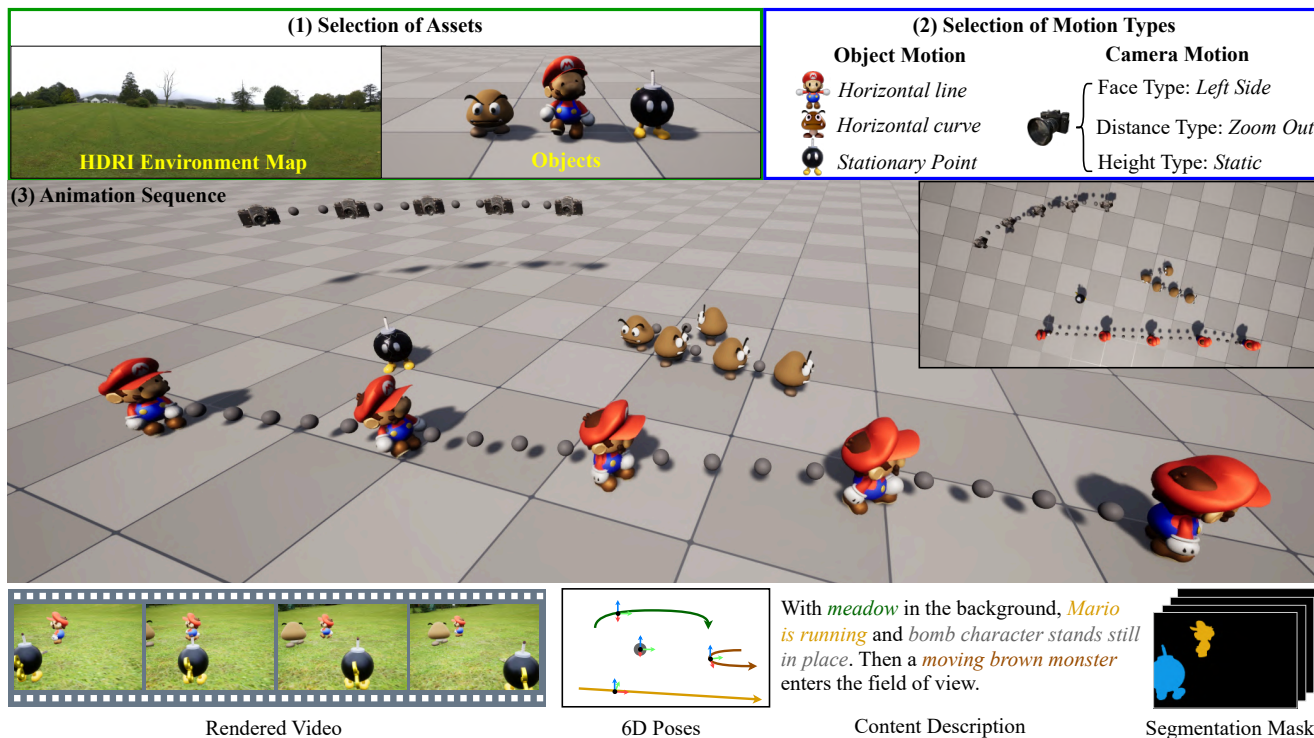


Figure 1. Generation pipeline of videos in the proposed **Synthetic Dataset for Free-Form Motion Control (SynFMC)**. The figure presents an example for generating synthetic video with three objects: (1) First, the HDRI environment map and objects matching the environment are selected as the assets. (2) Then, the motion types of objects and camera are selected for trajectory generation. (3) The center region shows the resulting 3D animation sequence used for rendering. The rendered video and annotations are demonstrated in the last row.

## Abstract

Controlling the movements of dynamic objects and the camera within generated videos is a meaningful yet challenging task. Due to the lack of datasets with comprehensive motion annotations, existing algorithms can not simultaneously control the motions of both camera and objects, resulting in limited controllability over generated contents. To address this issue and facilitate the research in this field, we introduce a **Synthetic Dataset for Free-Form Motion Control (SynFMC)**. The proposed SynFMC dataset includes di-

verse objects and environments and covers various motion patterns according to specific rules, simulating common and complex real-world scenarios. The complete 6D pose information facilitates models learning to disentangle the motion effects from objects and the camera in a video. To validate the effectiveness and generalization of SynFMC, we further propose a method, **Free-Form Motion Control (FMC)**. FMC enables independent or simultaneous control of object and camera movements, producing high-fidelity videos. Moreover, it is compatible with various personalized text-to-image (T2I) models for different content styles.

Extensive experiments demonstrate that the proposed *FMC* outperforms previous methods across multiple scenarios.

## 1. Introduction

Controlling motion dynamics in video generation has received increasing attention recently [9, 10, 16, 18, 19, 21, 42, 45, 46, 52, 61], as this capability enables better customization and plays a crucial role in many applications. For example, in filmmaking, directors meticulously choreograph the movements of both actors and the camera. Consequently, precise control over object and camera motions in video offers creative flexibility, enabling even non-professionals to create compelling visuals.

Despite recent progress, challenges remain in this field. A key limitation is *the lack of high-quality datasets with comprehensive motion annotations*. For controlling object movement [4, 20, 23, 26, 34, 43, 46, 47, 54, 60], the motion is primarily annotated as the trajectory in image space [46, 54]. This annotation, however, intertwines the dynamics of both objects and the camera. For example, a rightward trajectory could represent either a stationary camera with a moving object or a static object with a left-moving camera. Besides, existing commonly used datasets [50, 57, 63] for learning camera motion mainly focus on scenes with minimal object dynamics. Some human-centric synthetic datasets [3, 45, 51, 55] provide ground truth for both human subjects and camera motions within a global coordinate system, yet exhibit limited motion diversity and category variety. Another significant challenge is the absence of methods capable of jointly controlling both object and camera movements. For example, approaches like MotionZero [4] only animate objects within a restricted range [17, 23, 47], while methods like CameraCtrl [10] exclusively target camera motion [1, 14, 48]. MotionCtrl [46] recently attempts to train separate modules for object and camera control in a two-stage process. However, without access to video data containing complete 6D pose annotations for both elements, it struggles to achieve reliable, synchronized control of objects and cameras within the same scene.

To enable free-form control of camera and object dynamics, a dataset with comprehensive pose annotations of both is essential. However, acquiring such data in real world is challenging and typically requires specialized equipment and expertise. To address this, we introduce a **S**ynthetic dataset for **F**ree-Form **M**otion **C**ontrol (*SynFMC*). Designed with an emphasis on quality and diversity, the dataset includes a rich array of animated object assets across various categories, along with diverse HDRI (High Dynamic Range Imaging) environment maps. A rule-based generation strategy is implemented to create trajectories for both objects and the camera, as shown in Figure 1. This strategy encompasses basic patterns and simulates



Figure 2. Example videos generated by our method *FMC* trained on the proposed *SynFMC* dataset, showing its adaptability with different personalized T2I models [29, 38, 41].

challenging cinematographic shots. To enhance realism, essential attributes for each object asset, such as living environment, types of speed and size, are annotated using a Multimodal Large Language Model (MLLM) [5] and manual labeling, facilitating the generation of plausible motion paths. The *SynFMC* dataset also provides detailed annotations, including 6D pose information of objects and camera, instance segmentation maps, depth maps, and comprehensive descriptions of content and motion, supporting a wide range of research fields.

To further validate the effectiveness of the proposed *SynFMC* dataset and address the limitations of previous methods, we propose a *Free-Form Motion Control (FMC)* method. *FMC* mainly includes two components: Camera Motion Controller (CMC) and Object Motion Controller (OMC). Unlike previous methods [46, 54], our approach leverages complete pose annotations of both camera and objects to disentangle global (camera) and local (object) dynamics. As shown in Figure 2, *FMC* is adaptable to various personalized Text-to-Image (T2I) models, producing high-fidelity results across a range of styles. In addition, *FMC* provides flexible user interfaces for motion control. Users can simultaneously input trajectories for objects and camera by simply drawing curves or by specifying motion types for each (as detailed in Sec. 3.3), which are used by a rule-based strategy to generate their trajectories accordingly.

In summary, our main contributions are as follows:

- To the best of our knowledge, the *SynFMC* dataset is the first to provide 6D pose annotations for both camera and objects. Its diverse scenes and complex motion patterns provide models with valuable resources for learning the dynamics of multiple objects and the camera.
- The proposed *FMC* method enables joint or independent control of camera and object motions in video generation, achieving high-quality results across diverse scenes.
- Extensive experiments demonstrate that *FMC*, trained on *SynFMC* dataset, generates videos of superior quality compared to state-of-the-art methods.

Table 1. Comparison of the proposed *SynFMC* with existing datasets. The object/camera motion pattern columns apply only to synthetic datasets. “Limited Movement” means that motion is restricted to a limited range. In addition to offering a rich variety of object categories, *SynFMC* outperforms in both motion pattern variety and comprehensive pose annotations for camera and objects.

Dataset	Clips	Source	Category	Object Motion Pattern	Camera Motion Pattern	Camera Pose Annotation	Object Motion Annotation
RealEstate10K [63]	65K	Real	Real Estate	-	-	Fitting	×
MVImgNet [57]	220K	Real	<b>Common</b>	-	-	Fitting	×
VideoHD [54]	75K	Real	<b>Common</b>	-	-	×	Optical Flow
MotionCtrl [46]	<b>240K</b>	Real	<b>Common</b>	-	-	×	Optical Flow
HumanVid-Real [45]	20K	Real	Human	-	-	Fitting	2D Human Pose
BEDLAM [3]	10K	Synthetic	Human	Limited Movement	Static	<b>Ground Truth</b>	3D Human Pose
SynBody [51]	27K	Synthetic	Human	Limited Movement	Static	<b>Ground Truth</b>	3D Human Pose
HumanVid-Syn [45]	100K	Synthetic	Human	Limited Movement	Limited Patterns	<b>Ground Truth</b>	3D Human Pose
<i>SynFMC</i> (ours)	26K	Synthetic	<b>Common</b>	<b>Diverse Patterns</b>	<b>Diverse Patterns</b>	<b>Ground Truth</b>	<b>Object Pose</b>

## 2. Related Work

**Text-To-Video Generation.** In text-to-video (T2V) models [8, 9, 12, 13, 22, 35, 36, 59], spatial modules determine the visual content while temporal modules control motion dynamics. However, lots of online videos are of low-quality characterized by motion blur and watermarks. Recently, Animatediff [9] incorporates the Domain Adapter into spatial modules to alleviate this issue. Moreover, it is highly compatible with other network modules [30, 53, 58], leading to the widespread usage within the community.

**Dataset with Motion Annotations.** For object control, most datasets [46, 54] focus on operation within the image space. However, the motions of camera and object are coupled in this space, while limiting the movement scope. On the other hand, only a few real datasets [50, 57, 63] contain camera pose information, and these primarily focus on static scenes without dynamic objects. Some synthetic datasets [3, 45, 51, 55] provide pose annotations for both objects and camera. Nevertheless, the 3D assets in these works are primarily focused on humans, resulting in limited category diversity. More discussions are in Sec 3.1.

**Motion Control Methods.** Most existing works [10, 17, 48, 60] can only control either object motion or viewpoint change. For methods that achieve manipulation over the motions of both the camera and objects, Direct-a-Video [50] can only simulate basic movements and simultaneous control in MotionCtrl [46] often results in suboptimal outcomes as noted in its study [46]. More discussions are in Sec 4.

## 3. SynFMC Dataset

### 3.1. Comparison with Existing Datasets

There is currently a lack of datasets that contain 6D poses for both objects and the camera [45, 57, 63]. As shown in Table 1, only a few real datasets [57, 63] provide estimated camera pose annotations, and they are primarily limited to scenes without dynamic objects due to the suboptimal performance of estimation methods [31, 37, 62]. To alleviate this, some methods [46, 54] use in-the-

wild videos with image-space object trajectory inferred by optical flow models [62], but this way couples object and camera motions, resulting in ambiguities.

In contrast, synthetic datasets can conveniently obtain pose information [3, 45, 51, 55]. As shown in Table 1, most efforts focus on animating human. For example, HumanVid [45] constructs synthetic videos for controlling both human animation and camera motion. However, other common object categories remain underexplored. Furthermore, these datasets are limited to small human movements and simple camera motion patterns, restricting the model’s ability to learn complicated dynamic.

To effectively disentangle object and camera motion dynamics in video, it is essential to construct a new dataset with comprehensive object and camera poses. However, this is highly challenging in real world. First, capturing videos with complex, irregular object and camera motions is extremely difficult, typically requiring specialized equipment and expertise. Then, obtaining accurate pose estimation is difficult. Devices capable of capturing 6D poses for camera or objects are expensive and difficult to operate. Some studies [46, 63] attempt to obtain camera pose via estimation models. However, existing algorithms [37, 62] are time-intensive and often struggle with monocular videos containing dynamic objects. Besides, inferring 6D poses for general objects remains challenging. To address these limitations, we introduce *SynFMC*, a synthetic dataset generated using *Unreal Engine* [39], containing animations with diverse motion patterns and complete annotations.

### 3.2. Overview of *SynFMC* Dataset

*SynFMC* contains 26K videos divided into four groups: 6K *static single-object*, 6K *static multi-object*, 8K *dynamic single-object*, and 6K *dynamic multi-object*. *Static* means fixed object locations in world space while the camera remains movable. For diversity, the dataset includes common objects across various categories, such as humans, animals, plants and vehicles, as well as a wide range of environments like streets, grasslands, skies, oceans, *etc.* Additionally,



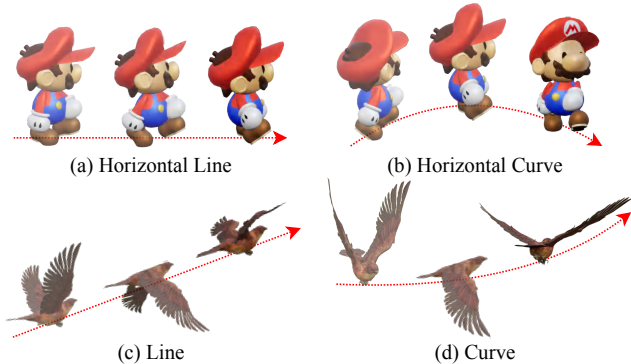


Figure 3. Object motion types. The line/curve in (c)/(d) are not limited in the horizontal plane. The trajectory of *stationary point* is not presented in the figure, which is a fixed point in the space.

*SynFMC* has diverse and complex multi-object and camera movements, covering not only basic motions but also shots that are challenging to achieve in real-world settings. Object assets are annotated with attributes such as speed and size by human annotators with the aid of MLLM [5] to ensure realistic motion simulation.

- **Video Annotations.** The proposed *SynFMC* dataset offers thorough annotations, including pose information for both objects and the camera, instance segmentation masks, depth maps, and detailed descriptions of content and motion, broadening its applicability across various research fields.

### 3.3. Data Generation Pipeline

The key stages in the generation pipeline are outlined below.

- **Asset Collection and Annotation.** We collect a diverse set of 3D assets, including HDRI environment maps and animated objects, to enrich rendered content. The HDRI maps, used as backgrounds, span five types: *ground*, *near ground*, *sky*, *water surface*, and *underwater*, collected from PolyHaven [25]. For object assets, we select 6K resources with available animations from Objaverse-LVIS [7], Objaverse-XL [6], Mixamo [24], *etc.*, covering a diverse range of categories. Low-quality assets are filtered out by human annotators. Then InternVL [5] is used to query basic properties of the object, such as class name, habitat, speed, and size category. This information is then verified or corrected by human annotators, who also label the motion type and provide a description for each animation.

- **Object Motion.** To create realistic motions, we design trajectories based on Bézier curves, where the rotations are derived from tangent and normal vectors along the curve. Examples of each motion type are shown in Figure 3. In implementation, the locations of control points are constrained within a reasonable range based on the object’s speed type.

- **Camera Motion.** For camera simulation, we decompose the relative movement of camera to object into 3 aspects: *viewpoint type*, *distance type*, and *height type*, see Figure 4. (a) *Viewpoint type* controls the orientation of the camera

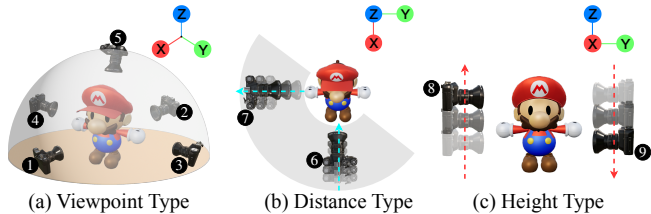


Figure 4. Decomposition of camera motion. We decompose the camera motion into three aspects. (a) *Viewpoint type* indicates the orientation of the camera relative to the object. ①-⑤ present front/back, left/right side and top perspectives. (b) *Distance type* and (c) *Height type* determine horizontal and vertical distance between the camera and the object respectively. ⑥-⑨ are zoom in/out and up/down respectively. The “static” types are omitted in (b) and (c), which stand for fixed distances.

relative to the object: 1) front/back: camera captures objects from front/back view; 2) left/right side: camera captures objects from left/right side; 3) top: camera captures objects from top view. In implementation, viewpoint types are randomly assigned to selected key frames, with viewpoints for other frames determined through interpolation, enabling the camera’s range of motion to encompass all orientations around the object. (b) *Distance type* controls the horizontal distance between the camera and objects: 1) zoom in/out and 2) static. (c) *Height type* controls the vertical distance between the camera and objects: 1) up/down and 2) static. To keep the object within the camera’s view without anchoring it at the image center, the camera orientation is adjusted to focus on a random offset from the object’s centroid.

- **Generation of Multi-Object Scenes.** First, objects from the same environment with comparable sizes and speeds are selected. Next, we generate trajectories for each object. Specifically, the first object’s trajectory is created using the way described earlier, while the trajectories of others are generated based on the previous object’s path, following a similar way used in camera motion simulation. For camera motion, we randomly select an object as the tracking target in each segment, with the trajectory generated using the same method as previously outlined.

- **Rendering.** This stage creates synthetic videos based on selected assets and motion types of objects and the camera as shown in Figure 1. Specifically, for each segment in the video, we randomly select animations for the chosen objects and generate trajectories according to its annotated motion type. Similarly, random combinations of camera motion types are applied across different segments, allowing the generated videos to encompass a wide range of motion patterns as in real-world scenarios. Finally, the selected assets (background and objects) and poses of the camera and objects are imported into *Unreal Engine* [39] to get 3D animation sequence for rendering.



Table 2. Comparison of the proposed FMC with existing methods. *FMC* excels in more flexible inputs and a wide range of motion patterns.

Methods	Motion Condition	Object Control	Camera Control	Dataset
AnimateDiff [9]	$\times$	$\times$	Limited Patterns	Dataset for Specific Motion Pattern
CameraCtrl [10]	<b>Camera Pose</b>	$\times$	<b>Diverse Patterns</b>	RealEstate10K [63]
VideoComposer [43]	Image Space Trajectory	Entanglement	Entanglement	LAION-400M [32] + WebVid [2]
DragNUWA [54]	Image Space Trajectory	Entanglement	Entanglement	WebVid+ VideoHD [54]
Direct-a-Video [50]	Image Space Trajectory + Camera Type	Entanglement	Limited Patterns	MovieShot [28]
MotionCtrl [46]	Image Space Trajectory + <b>Camera Pose</b>	Entanglement	<b>Diverse Patterns</b>	RealEstate10K + WebVid
<b>FMC (ours)</b>	<b>Object Pose + Camera Pose</b>	<b>Diverse Patterns</b>	<b>Diverse Patterns</b>	<i>SynFMC</i> (ours)

## 4. The Proposed Approach

Given  $N$ -length camera poses  $\mathcal{C}_{RT} = RT_{cam}^{1:N}$ , object poses  $\mathcal{O}_{RT} = \left\{ RT_{obj_i}^{1:N} \right\}_{i=1}^{N_o}$  of  $N_o$  objects in the global coordinate system, and content description  $\mathcal{C}_p$ , we aim to generate the video that reveals correct motion in real world.

As shown in Table 2, most methods cannot independently or jointly control object and camera movements. For example, AnimateDiff [9] and CameraCtrl [10] only support camera control, while other methods [43, 46, 50, 54] handle image-space trajectories for object motion control, often facing motion entanglement issues. Although Direct-a-Video [50] introduces several camera types and allows explicit control, it is limited to simple motion patterns. MotionCtrl [46], the closest to ours, trains two motion modules separately but lacks comprehensive pose annotations, resulting in suboptimal simultaneous control of camera and object motions. MotionCtrl’s object motion control module can only handle image-space trajectory, without accounting for orientation and distance. Additionally, MotionCtrl simply applies standard diffusion loss [11] when training motion modules, which further hinders its ability to disentangle camera and object motions within a video. *FMC* trained on *SynFMC* introduces Camera Motion Controller (CMC) and Object Motion Controller (OMC) to address these limitations. Among them, OMC receives 6D pose and coarse mask of the object to perceive its spatial location and orientation, thereby achieving a realistic appearance from various viewpoints. Additionally, the training objectives enable *FMC* to disentangle the motion effects of objects and the camera in the video, allowing independent or simultaneous control of camera and object motions.

- **Preliminary.** 1) During training, T2V diffusion models [9, 12, 13, 36, 56, 59] add Gaussian noise  $\epsilon$  to image sequence  $\mathbf{z}_0^{1:N}$ , resulting in noisy latents  $\mathbf{z}_t^{1:N}$  at  $t$  time step. Network  $\varepsilon_\theta$  then is trained to infer the injected noise from current latents. 2) AnimateDiff [9] uses Domain Adapter to adapt spatial modules to low-quality content. We apply this to bridge the synthetic-real video domain gap. 3) Following CameraCtrl [10], we use plücker embedding to represent camera pose for geometric interpretation.

### 4.1. Free-Form Motion Control

The overall architecture is shown in Figure 5. We train the proposed *FMC* (*Free-Form Motion Control*) in 3 stages.

First, LoRA modules [15] are injected into the spatial blocks as Domain Adapter [9], learning the rendered content. The temporal modules remain inactive at this stage, and images are randomly sampled from synthetic data. Next, CMC parameters are updated to learn camera motion, with LoRA weights from the previous step loaded and temporal modules introduced to the model. Finally, OMC is trained to decouple object dynamics from camera motion, while other parameters are frozen.

- **Construction of Training Data.** We randomly sample frames from the original video at uniform intervals and obtain the corresponding object masks. Since *SynFMC* has detailed descriptions of the background, objects and their actions for each time step, video text descriptions can be automatically generated by specific templates. Then, these labels with pose information of camera and objects are used for training motion controllers.

- **Camera Motion Controller (CMC).** It consists of two parts as shown in Figure 5. Camera Encoder receives the initial camera pose (translation values are set to 0) and plücker embeddings of subsequent frames. The introduction of the initial pose helps to determine the perspective at the start time. Then, the outputs are processed by Camera Adapter to modulate the features in temporal blocks. Due to the dynamic of the background being only affected by camera motion, *camera loss*  $L_{cam}$  is applied in this stage:

$$L_{cam} = E_{\mathbf{z}_0^{1:N}, t, \epsilon, \mathcal{C}_p, \mathcal{C}_{RT}} [\mathcal{M}_{bg} \|\varepsilon_{\theta, \theta_c}(\mathbf{z}_t^{1:N}, t, \mathcal{C}_p, \mathcal{C}_{RT}) - \epsilon\|^2 + \lambda_c \|\varepsilon_{\theta, \theta_c}(\mathbf{z}_t^{1:N}, t, \mathcal{C}_p, \mathcal{C}_{RT}) - \epsilon\|^2], \quad (1)$$

where  $\theta_c$  is the parameters of CMC.  $\mathcal{M}_{bg}$  is background mask and  $\lambda_c$  is the weighting factor.  $L_{cam}$  makes camera motion more accurate by concentrating on the background.

- **Object Motion Controller (OMC).** The Object Encoder of OMC receives 6D object pose information to adjust the features in spatial modules from several downsample blocks [29, 46]. Specifically, the poses relative to the camera in each frame are duplicated within the respective object region while the others are set to 0. Then, the pose features concatenated with the foreground mask are fed to OMC. In this manner, the poses from different objects can be aggregated in a single input. Besides, we leverage the Gaussian blur kernel centered at the object centroid to avoid users offering precise masks. Then, the outputs from OMC are multiplied by the coarse masks and added to the spatial features in the main branch, preventing to impair the

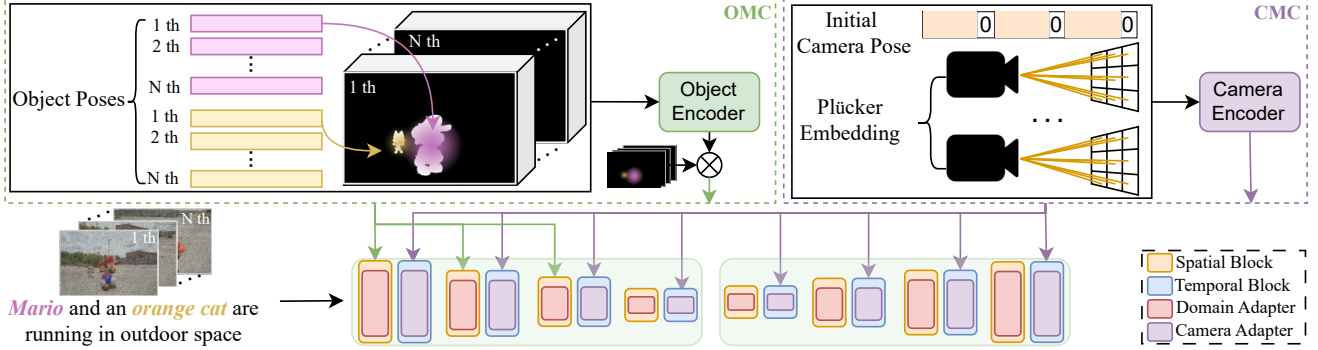


Figure 5. The architecture of *FMC*. In the first stage, we randomly sample the images from synthetic videos and update the parameters from injected *Domain Adapter*. Next, the modules from CMC are learned. It consists of two parts: *Camera Encoder* and *Camera Adapter*, where the Camera Adapter is introduced into the temporal modules. Finally, we train the *Object Encoder* from OMC. It receives the object pose features, which are repeated in the corresponding object region. We use Gaussian blur kernel centered at the centroid to prevent the need of precise masks. Then, the output is multiplied by the coarse masks to modulate the features in the main branch.

background content. During inference, the size of the kernel can be approximated based on the object’s size (specified by the user) and its distance from the camera. *object loss*  $L_{obj}$  is applied to make OMC focus on the object region:

$$L_{obj} = E_{\mathbf{z}_0^{1:N}, t, \epsilon, \mathbf{C}_p, \mathcal{C}_{RT}, \mathcal{O}_{RT}} [ \mathcal{M}_{fg} \|\varepsilon_{\theta, \theta_c, \theta_o}(\mathbf{z}_t^{1:N}, t, \mathbf{C}_p, \mathcal{C}_{RT}, \mathcal{O}_{RT}) - \epsilon\|^2 + \lambda_o \|\varepsilon_{\theta, \theta_c, \theta_o}(\mathbf{z}_t^{1:N}, t, \mathbf{C}_p, \mathcal{C}_{RT}, \mathcal{O}_{RT}) - \epsilon\|^2 ], \quad (2)$$

where  $\theta_o$  indicates the parameters from OMC.  $\mathcal{M}_{fg}$  is foreground mask and  $\lambda_o$  is the weighting factor.  $L_{obj}$  improves the appearance quality of dynamic objects.

## 5. Experiments

• **Implementation Details.** The proposed *FMC* is based on AnimateDiff V3 [9], trained with 16-length  $256 \times 384$  videos, Adam optimizer with a learning rate of  $1e^{-4}$ . Domain Adapter is trained with 8K iterations in a batch size of 128. CMC and OMC are trained with 50K iterations with a batch size of 8.  $\lambda_c$  and  $\lambda_o$  are set to 0.6 and 0.3.

• **Evaluation Metrics.** Following [9, 46], we use FID [33] to evaluate visual quality, FVD [40] for temporal coherence, and CLIPSIM [27] to measure semantic similarity with text. For camera motion, we follow [10] to use CamTransErr and CamRotErr. For object motion, ObjTransErr and ObjRotErr are introduced. We first use depth estimation model [49] to obtain the depth at object centroid and determine its global position based on camera pose, then fit a trajectory curve to find tangent and normal vectors at each time step, allowing for rotation derivation. Given scale information, we apply appropriate scaling to the translation error calculation.

### 5.1. Comparisons with State-of-the-Art Methods

We first compare independent control over camera motion and object motion, as in previous methods [10, 46]. Then, we demonstrate *FMC*’s superior performance in simultaneous control. Finally, we showcase additional exam-

Table 3. Quantitative comparison of our proposed method *FMC* with AnimateDiff [9], CameraCtrl [10], and MotionCtrl [46].

Method	AnimateDiff	CameraCtrl	MotionCtrl	<i>FMC</i> (ours)
FID ↓	149.61	137.96	<b>125.52</b>	133.42
FVD ↓	868.97	<b>805.25</b>	952.31	846.51
CLIPSIM ↑	29.33	29.21	26.83	<b>31.01</b>
CamTransErr ↓	-	18.16	<b>17.84</b>	18.12
CamRotErr ↓	-	<b>0.94</b>	1.11	1.03
ObjTransErr ↓	-	-	80.66	<b>42.25</b>
ObjRotErr ↓	-	-	1.77	<b>0.96</b>

ples across different scenes to validate the effectiveness of *SynFMC* and *FMC*.

• **Independent Control of Camera Motion.** MotionCtrl [46] and CameraCtrl [10] are selected for this comparison as they accept explicit camera information. In Figure 6(a), we simulate two camera motions and scale the translation to fit the input range required by these methods. *FMC* and the compared methods effectively reflect the input conditions. The CamTransErr & CamRotErr in Table 3 also show that *FMC* achieves comparable results in controlling camera.

• **Independent Control of Object Motion.** For object control, we compare with MotionCtrl [46] and Direct-a-Video [50]. For these methods, we project the global trajectory into image space using camera and object pose information. For our *FMC*, the camera pose condition is set to identity matrices as static camera. As shown in Figure 6(b), the compared methods fail to maintain a stationary camera (showing dynamic movement in the background), indicating that image space trajectories entangle the object and camera motions. For example, the 2nd example of Figure 6(b), the result of Direct-a-Video [50] shows the change of flower location, which is caused by dynamic camera. In contrast, our method effectively alleviates this issue by incorporating static camera poses as constraints.

• **Simultaneous Control of Camera and Object Motions.** We explore the combination of both camera and object control signals. Since Direct-a-Video [50] supports only



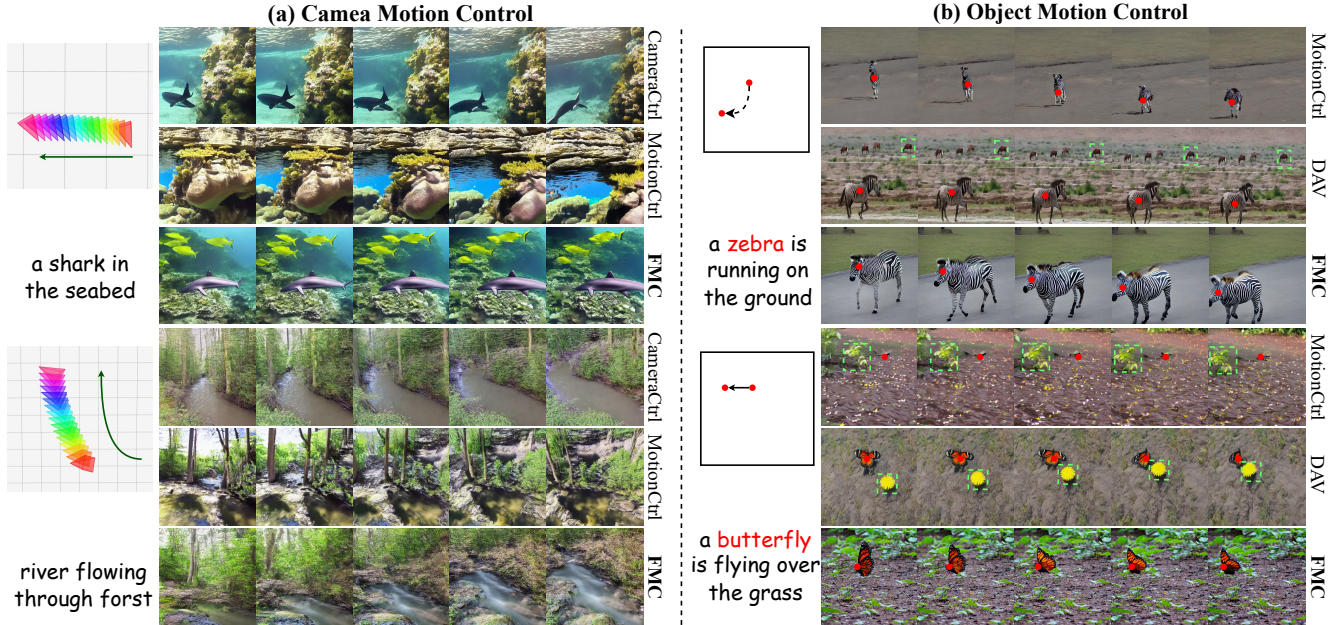


Figure 6. Independent control over camera and object motions. The results in (a) reveal that all methods [10, 46] effectively reflect the input conditions. For object motion control, the compared methods [46, 50] fail to maintain a stationary camera. As shown in green boxes from (b), the camera effect causes the dynamic in the background (e.g., movement of flower in row 5).

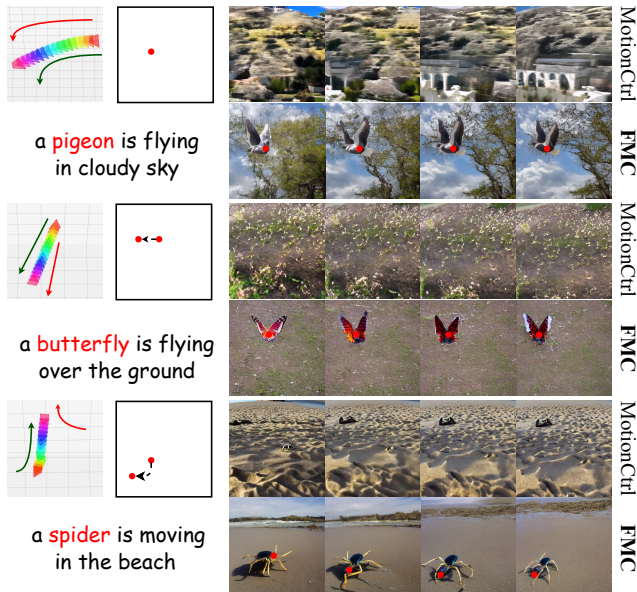


Figure 7. Simultaneous control over camera and object motions. MotionCtrl [46] struggles to generate realistic object dynamics, causing objects to disappear from view, whereas our *FMC* achieves high-quality simultaneous control.

basic camera motion, we choose MotionCtrl [46] as the comparison method. We randomly simulate movements for both the object and the camera, resulting in varied image-space trajectories. As shown in Figure 7, videos generated by *FMC* more faithfully align with the specified conditions. While MotionCtrl captures the camera’s motion, it struggles to generate realistic object dynamics.

Table 4. User study in quality, text similarity, and motion accuracy.

Method	CameraCtrl [10]	MotionCtrl [46]	<i>FMC</i> (ours)
Quality Score	0.88	0.89	<b>0.91</b>
Text Similarity Score	0.84	0.81	<b>0.95</b>
Camera Motion Score	<b>0.95</b>	0.93	<b>0.95</b>
Object Motion Score	-	0.53	<b>0.98</b>

These results demonstrate the effectiveness of our method in achieving simultaneous control of camera and object motions. The object error metrics in Table 3 show that our method achieves better results in object motion control. Additionally, *FMC* achieves higher scores in user study, as shown in Table 4, outperforming previous methods in quality and fidelity for both camera and object motions.

Figure 8 shows video generation results across 4 different cases: *static single-object*, *dynamic single object*, *static multi-object*, and *dynamic multi-object*. Thanks to the diversity and complexity of camera and motion motion patterns in *SynFMC*, *FMC* effectively learns a range of diverse, advanced, and complex shots. In the 2nd row of Figure 8, for example, the camera initially captures the person from the front and then follows from behind. The last two rows demonstrate the performance in multi-object scenarios, where the relative motion between objects and the camera conforms closely to the input conditions.

## 5.2. Ablation Study

• **SynFMC Dataset.** To validate the effectiveness of complete camera and object pose annotations in *SynFMC* and evaluate the dataset generalization, we train MotionCtrl [46] on it, adapting the annotations to its input format. We



Table 5. Quantitative results in ablation study.

Metrics	CamTransErr	CamRotErr	ObjTransErr	ObjRotErr
MotionCtrl (w/o $C_{RT}$ )	18.24	1.08	78.82	1.65
MotionCtrl (w/ $C_{RT}$ )	18.24	1.08	55.33	1.26
FMC (w/o $L_{cam}$ )	20.35	1.19	-	-
FMC (w/o $L_{obj}$ )	<b>18.12</b>	<b>1.03</b>	46.62	1.15
FMC	<b>18.12</b>	<b>1.03</b>	<b>42.25</b>	<b>0.96</b>



Figure 8. Simultaneous control results of *FMC* in different cases. The complicated case in row 2 shows that our method learns complex shot, where the camera first captures a skier from the front and then follows him from behind.



Figure 9. Simultaneous control results of MotionCtrl [46] trained on *SynFMC* without and with camera pose during training.

first train the camera module, then optimize the object module in two ways: without camera poses, as in [46], and with camera poses, as our *FMC*. As shown in Figure 9, incorporating known camera poses when optimizing object module allows the object to follow the input trajectory more accurately, reducing the risk of it leaving the field of view. Object motion errors in Table 5 further highlight the benefits of using complete camera and object pose annotations.

- **OMC.** As shown in the first two rows of Figure 10 and object motion errors in Table 5, *FMC* outperforms MotionCtrl [46] trained on *SynFMC* in motion accuracy. This improvement is brought by OMC’s ability to process 6D poses, generating more realistic object appearances based on orientation and object’s distance from the camera, reflected by the size of coarse masks. In contrast, MotionCtrl’s object motion control module can only handle 2D image-space trajectories without pose and distance information, limiting alignment accuracy with the input.

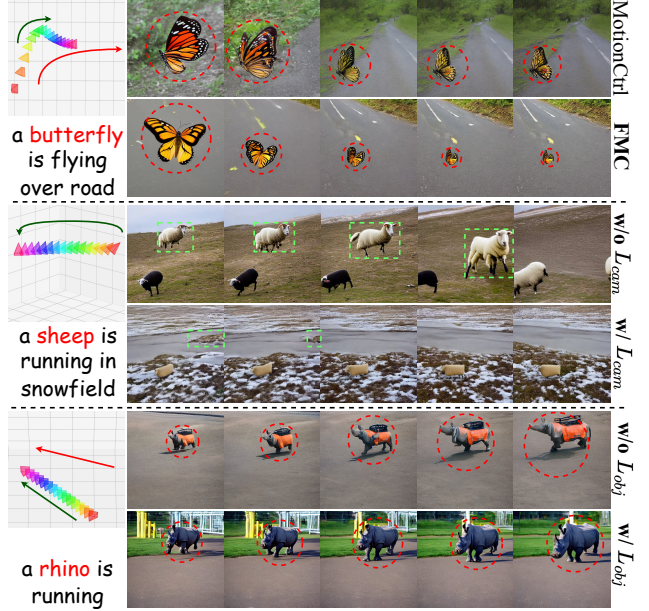


Figure 10. Results of different settings in the ablation study. The first row is MotionCtrl [46] trained on *SynFMC*.

- **Training Objectives.** We conduct two experiments to assess the impact of  $L_{cam}$  in Eq. (1) and  $L_{obj}$  in Eq. (2). First, we train CMC using only the standard diffusion loss [11, 44]. As shown in the 3rd row of Figure 10, model without  $L_{cam}$  tends to shift foreground objects to achieve similar relative motion, which does not accurately match the input pose. The camera motion error in Table 5 underscores the effectiveness of  $L_{cam}$ . Similarly, training OMC without  $L_{obj}$  leads to undesired object appearances, as shown in the 5th row of Figure 10, with object motion error in Table 5 confirming the benefit of  $L_{obj}$ .

- **Adaptability with Different T2I Personalized models.** As shown in Figure 2, *FMC* can be adapted to various personalized backbones [29, 38, 41], showing that our proposed dataset *SynFMC* and corresponding training strategy do not impair the model’s original generative capabilities.

## 6. Conclusion

This work introduces *SynFMC*, a dataset with comprehensive pose information and diverse assets, offering both standard and complex shots that are difficult to capture in real life, with trajectories resembling real-world scenarios. With *SynFMC*, the proposed method *FMC* enables independent or joint control of object and camera motions within a single video. Experimental results demonstrate the effectiveness of both *SynFMC* dataset and *FMC*.

**Limitations.** Our method’s ability to control complex motions of multiple objects remains limited. Better metrics are needed to more accurately evaluate object motion. In the future, additional input modalities, *e.g.*, images, are desired to customize motion videos for reference subjects.

## References

- [1] Sherwin Bahmani, Ivan Skorokhodov, Aliaksandr Siarohin, Willi Menapace, Guocheng Qian, Michael Vasilkovsky, Hsin-Ying Lee, Chaoyang Wang, Jiaxu Zou, Andrea Tagliasacchi, David B. Lindell, and Sergey Tulyakov. VD3D: taming large video diffusion transformers for 3d camera control. *arXiv*, 2025.
- [2] Max Bain, Arsha Nagrani, Gül Varol, and Andrew Zisserman. Frozen in time: A joint video and image encoder for end-to-end retrieval. In *ICCV*, 2021.
- [3] Michael J. Black, Priyanka Patel, Joachim Tesch, and Jinlong Yang. BEDLAM: A synthetic dataset of bodies exhibiting detailed lifelike animated motion. In *CVPR*, 2023.
- [4] Changgu Chen, Junwei Shu, Lianggangxu Chen, Gaoqi He, Changbo Wang, and Yang Li. Motion-Zero: Zero-shot moving object control framework for diffusion-based video generation. *arXiv*, 2024.
- [5] Zhe Chen, Jiannan Wu, Wenhai Wang, Weijie Su, Guo Chen, Sen Xing, Muyan Zhong, Qinglong Zhang, Xizhou Zhu, Lewei Lu, Bin Li, Ping Luo, Tong Lu, Yu Qiao, and Jifeng Dai. InternVL: Scaling up vision foundation models and aligning for generic visual-linguistic tasks. In *CVPR*, 2024.
- [6] Matt Deitke, Ruoshi Liu, Matthew Wallingford, Huong Ngo, Oscar Michel, Aditya Kusupati, Alan Fan, Christian Laforte, Vikram Voleti, Samir Yitzhak Gadre, Eli VanderBilt, Aniruddha Kembhavi, Carl Vondrick, Georgia Gkioxari, Kiana Ehsani, Ludwig Schmidt, and Ali Farhadi. Objaverse-xl: A universe of 10m+ 3d objects. In *NeurIPS*, 2023.
- [7] Matt Deitke, Dustin Schwenk, Jordi Salvador, Luca Weihs, Oscar Michel, Eli VanderBilt, Ludwig Schmidt, Kiana Ehsani, Aniruddha Kembhavi, and Ali Farhadi. Objaverse: A universe of annotated 3d objects. In *CVPR*, 2023.
- [8] Jiahua Dong, Wenqi Liang, Hongliu Li, Duzhen Zhang, Meng Cao, Henghui Ding, Salman Khan, and Fahad Khan. How to continually adapt text-to-image diffusion models for flexible customization? In *NeurIPS*, 2024.
- [9] Yuwei Guo, Ceyuan Yang, Anyi Rao, Yaohui Wang, Yu Qiao, Dahua Lin, and Bo Dai. AnimateDiff: Animate your personalized text-to-image diffusion models without specific tuning. In *ICLR*, 2024.
- [10] Hao He, Yinghao Xu, Yuwei Guo, Gordon Wetzstein, Bo Dai, Hongsheng Li, and Ceyuan Yang. CameraCtrl: Enabling camera control for text-to-video generation. *arXiv*, 2024.
- [11] Jonathan Ho, Ajay Jain, and Pieter Abbeel. Denoising diffusion probabilistic models. In *NeurIPS*, 2020.
- [12] Jonathan Ho, William Chan, Chitwan Saharia, Jay Whang, Ruiqi Gao, et al. Imagen Video: High definition video generation with diffusion models. *arXiv*, 2022.
- [13] Jonathan Ho, Tim Salimans, Alexey A. Gritsenko, William Chan, Mohammad Norouzi, and David J. Fleet. Video diffusion models. In *NeurIPS*, 2022.
- [14] Chen Hou, Guoqiang Wei, Yan Zeng, and Zhibo Chen. Training-free camera control for video generation. *arXiv*, 2024.
- [15] Edward J. Hu, Yelong Shen, Phillip Wallis, Zeyuan Allen-Zhu, Yuanzhi Li, Shean Wang, Lu Wang, and Weizhu Chen. LoRA: Low-rank adaptation of large language models. In *ICLR*, 2022.
- [16] Teng Hu, Jiangning Zhang, Ran Yi, Yating Wang, Hongrui Huang, Jieyu Weng, Yabiao Wang, and Lizhuang Ma. MotionMaster: Training-free camera motion transfer for video generation. In *ACM MM*, 2024.
- [17] Yash Jain, Anshul Nasery, Vibhav Vineet, and Harkirat S. Behl. Peekaboo: Interactive video generation via masked-diffusion. In *CVPR*, 2024.
- [18] Hyeonho Jeong, Jinho Chang, Geon Yeong Park, and Jong Chul Ye. DreamMotion: Space-time self-similarity score distillation for zero-shot video editing. In *ECCV*, 2024.
- [19] Hyeonho Jeong, Geon Yeong Park, and Jong Chul Ye. VMC: video motion customization using temporal attention adaption for text-to-video diffusion models. In *CVPR*, 2024.
- [20] Yaowei Li, Xintao Wang, Zhaoyang Zhang, Zhouxia Wang, Ziyang Yuan, Liangbin Xie, Yuexian Zou, and Ying Shan. Image Conductor: Precision control for interactive video synthesis. *arXiv*, 2024.
- [21] Pengyang Ling, Jiazi Bu, Pan Zhang, Xiaoyi Dong, Yuhang Zang, Tong Wu, Huaian Chen, Jiaqi Wang, and Yi Jin. MotionClone: Training-free motion cloning for controllable video generation. *arXiv*, 2025.
- [22] Chang Liu, Xiangtai Li, and Henghui Ding. Referring image editing: Object-level image editing via referring expressions. In *CVPR*, 2024.
- [23] Wan-Duo Kurt Ma, John P. Lewis, and W. Bastiaan Kleijn. TrailBlazer: Trajectory control for diffusion-based video generation. *arXiv*, 2024.
- [24] Mixamo. <https://mixamo.com>, 2022.
- [25] PolyHaven. <https://polyhaven.com>, 2022.
- [26] Haonan Qiu, Zhaoxi Chen, Zhouxia Wang, Yingqing He, Menghan Xia, and Ziwei Liu. FreeTraj: Tuning-free trajectory control in video diffusion models. *arXiv*, 2024.
- [27] Alec Radford, Jong Wook Kim, Chris Hallacy, Aditya Ramesh, Gabriel Goh, Sandhini Agarwal, Girish Sastry, Amanda Askell, Pamela Mishkin, Jack Clark, Gretchen Krueger, and Ilya Sutskever. Learning transferable visual models from natural language supervision. In *ICML*, 2021.
- [28] Anyi Rao, Jiaye Wang, Linning Xu, Xuekun Jiang, Qingqiu Huang, Bolei Zhou, and Dahua Lin. A unified framework for shot type classification based on subject centric lens. In *ECCV*, 2020.
- [29] Robin Rombach, Andreas Blattmann, Dominik Lorenz, Patrick Esser, and Björn Ommer. High-resolution image synthesis with latent diffusion models. In *CVPR*, 2022.
- [30] Nataniel Ruiz, Yuanzhen Li, Varun Jampani, Yael Pritch, Michael Rubinstein, and Kfir Aberman. DreamBooth: Fine tuning text-to-image diffusion models for subject-driven generation. In *CVPR*, 2023.
- [31] Johannes L. Schönberger and Jan-Michael Frahm. Structure-from-motion revisited. In *CVPR*, 2016.
- [32] Christoph Schuhmann, Richard Vencu, Romain Beaumont, Robert Kaczmarczyk, Clayton Mullis, Aarush Katta, Theo Coombes, Jenia Jitsev, and Aran Komatsuzaki. LAION-400M: open dataset of clip-filtered 400 million image-text pairs. *arXiv*, 2021.

- [33] Maximilian Seitzer. pytorch-fid: FID Score for PyTorch, 2020.
- [34] Xiaoyu Shi, Zhaoyang Huang, Fu-Yun Wang, Weikang Bian, Dasong Li, Yi Zhang, Manyuan Zhang, Ka Chun Cheung, Simon See, Hongwei Qin, Jifeng Dai, and Hongsheng Li. Motion-I2V: Consistent and controllable image-to-video generation with explicit motion modeling. In *SIGGRAPH*, 2024.
- [35] Xincheng Shuai, Henghui Ding, Xingjun Ma, Rongcheng Tu, Yu-Gang Jiang, and Dacheng Tao. A survey of multimodal-guided image editing with text-to-image diffusion models. *arXiv*, 2024.
- [36] Uriel Singer, Adam Polyak, Thomas Hayes, Xi Yin, Jie An, Songyang Zhang, Qiyuan Hu, Harry Yang, Oron Ashual, Oran Gafni, Devi Parikh, Sonal Gupta, and Yaniv Taigman. Make-a-video: Text-to-video generation without text-video data. In *ICLR*, 2023.
- [37] Zachary Teed and Jia Deng. DROID-SLAM: deep visual SLAM for monocular, stereo, and RGB-D cameras. In *NeurIPS*, 2021.
- [38] Bradcatt: Toonyou. <https://civitai.com/models/30240/toonyou>, 2024.
- [39] Unreal Engine 5. <https://www.unrealengine.com/>, 2022.
- [40] Thomas Unterthiner, Sjoerd van Steenkiste, Karol Kurach, Raphaël Marinier, Marcin Michalski, and Sylvain Gelly. Towards accurate generative models of video: A new metric & challenges. *arXiv*, 2018.
- [41] Realistic Vision. <https://civitai.com/models/4201/realistic-vision-v20>, 2023.
- [42] Luozhou Wang, Guibao Shen, Yixun Liang, Xin Tao, Pengfei Wan, Di Zhang, Yijun Li, and Yingcong Chen. Motion inversion for video customization. *arXiv*, 2025.
- [43] Xiang Wang, Hangjie Yuan, Shiwei Zhang, Dayou Chen, Juniu Wang, Yingya Zhang, Yujun Shen, Deli Zhao, and Jingren Zhou. VideoComposer: Compositional video synthesis with motion controllability. In *NeurIPS*, 2023.
- [44] Zihao Wang. Score-based generative modeling through backward stochastic differential equations: Inversion and generation. In *ICLR*, 2021.
- [45] Zhenzhi Wang, Yixuan Li, Yanhong Zeng, Youqing Fang, Yuwei Guo, Wenran Liu, Jing Tan, Kai Chen, Tianfan Xue, Bo Dai, and Dahua Lin. HumanVid: Demystifying training data for camera-controllable human image animation. In *NeurIPS*, 2024.
- [46] Zhouxia Wang, Ziyang Yuan, Xintao Wang, Yaowei Li, Tianshui Chen, Menghan Xia, Ping Luo, and Ying Shan. MotionCtrl: A unified and flexible motion controller for video generation. In *SIGGRAPH*, 2024.
- [47] Jianzong Wu, Xiangtai Li, Yanhong Zeng, Jiangning Zhang, Qianyu Zhou, Yining Li, Yunhai Tong, and Kai Chen. MotionBooth: Motion-aware customized text-to-video generation. In *NeurIPS*, 2024.
- [48] Dejjia Xu, Weili Nie, Chao Liu, Sifei Liu, Jan Kautz, Zhangyang Wang, and Arash Vahdat. CamCo: Camera-controllable 3d-consistent image-to-video generation. *arXiv*, 2025.
- [49] Lihe Yang, Bingyi Kang, Zilong Huang, Zhen Zhao, Xiaogang Xu, Jiashi Feng, and Hengshuang Zhao. Depth anything V2. In *NeurIPS*, 2024.
- [50] Shiyuan Yang, Liang Hou, Haibin Huang, Chongyang Ma, Pengfei Wan, Di Zhang, Xiaodong Chen, and Jing Liao. Direct-a-Video: Customized video generation with user-directed camera movement and object motion. In *SIGGRAPH*, 2024.
- [51] Zhitao Yang, Zhongang Cai, Haiyi Mei, Shuai Liu, Zhaoxi Chen, Weiye Xiao, Yukun Wei, Zhongfei Qing, Chen Wei, Bo Dai, Wayne Wu, Chen Qian, Dahua Lin, Ziwei Liu, and Lei Yang. SynBody: Synthetic dataset with layered human models for 3d human perception and modeling. In *ICCV*, 2023.
- [52] Danah Yatim, Rafail Fridman, Omer Bar-Tal, Yoni Kasten, and Tali Dekel. Space-time diffusion features for zero-shot text-driven motion transfer. In *CVPR*, 2024.
- [53] Hu Ye, Jun Zhang, Sibio Liu, Xiao Han, and Wei Yang. IP-Adapter: Text compatible image prompt adapter for text-to-image diffusion models. *arXiv*, 2023.
- [54] Shengming Yin, Chenfei Wu, Jian Liang, Jie Shi, Houqiang Li, Gong Ming, and Nan Duan. DragNUWA: Fine-grained control in video generation by integrating text, image, and trajectory. *arXiv*, 2023.
- [55] Wanqi Yin, Zhongang Cai, Ruisi Wang, Fanzhou Wang, Chen Wei, Haiyi Mei, Weiye Xiao, Zhitao Yang, Qingping Sun, Atsushi Yamashita, Ziwei Liu, and Lei Yang. WHAC: world-grounded humans and cameras. *arXiv*, 2024.
- [56] Lijun Yu, Yong Cheng, Kihyuk Sohn, José Lezama, Han Zhang, Huiwen Chang, Alexander G. Hauptmann, Ming-Hsuan Yang, Yuan Hao, Irfan Essa, and Lu Jiang. MAGVIT: masked generative video transformer. In *CVPR*, 2023.
- [57] Xianggang Yu, Mutian Xu, Yidan Zhang, Haolin Liu, Chongjie Ye, Yushuang Wu, Zizheng Yan, Chenming Zhu, Zhangyang Xiong, Tianyou Liang, Guanying Chen, Shuguang Cui, and Xiaoguang Han. MVImgNet: A large-scale dataset of multi-view images. In *CVPR*, 2023.
- [58] Lvmin Zhang, Anyi Rao, and Maneesh Agrawala. Adding conditional control to text-to-image diffusion models. In *ICCV*, 2023.
- [59] Shiwei Zhang, Jiayu Wang, Yingya Zhang, Kang Zhao, Hangjie Yuan, Zhiwu Qin, Xiang Wang, Deli Zhao, and Jingren Zhou. I2VGen-XL: High-quality image-to-video synthesis via cascaded diffusion models. *arXiv*, 2023.
- [60] Zhenghao Zhang, Junchao Liao, Menghao Li, Long Qin, and Weizhi Wang. Tora: Trajectory-oriented diffusion transformer for video generation. *arXiv*, 2024.
- [61] Rui Zhao, Yuchao Gu, Jay Zhangjie Wu, David Junhao Zhang, Jiawei Liu, Weijia Wu, Jussi Keppo, and Mike Zheng Shou. MotionDirector: Motion customization of text-to-video diffusion models. In *ECCV*, 2023.
- [62] Wang Zhao, Shaohui Liu, Hengkai Guo, Wenping Wang, and Yong-Jin Liu. ParticleSfM: Exploiting dense point trajectories for localizing moving cameras in the wild. In *ECCV*, 2022.
- [63] Tinghui Zhou, Richard Tucker, John Flynn, Graham Fyffe, and Noah Snavely. Stereo magnification: learning view synthesis using multiplane images. *ACM TOG*, 2018.